

# Two- and three-photon absorption in a novel fluorene-based compound

Wenbo Ma (马文波)<sup>1</sup>, Yiqun Wu (吴谊群)<sup>1,2</sup>, Donghong Gu (顾冬红)<sup>1</sup>, and Fuxi Gan (干福熹)<sup>1</sup>

<sup>1</sup>Shanghai Institute of Optics and Fine Mechanics, Chinese Academy of Sciences, Shanghai 201800

<sup>2</sup>Lab of Functional Materials Heilongjiang University, Haerbin 150080

Received January 17, 2005

A novel symmetrical charge transfer fluorene-based compound 2,7-bis (4-methoxystyryl)-9, 9-bis (2-ethylhexyl)-9H-fluorene (abbreviated as BMOSF) was synthesized and its nonlinear absorption was investigated using two different laser systems: a 140-fs, 800-nm Ti:sapphire laser operating at 1-kHz repetition rate and a 38-ps, 1064-nm Nd:YAG pulsed laser operating at 10-Hz repetition rate, respectively. Unique nonlinear absorption properties in this new compound were observed that rise from multiphoton absorption. The nonlinear absorption coefficients were measured to be  $6.02 \times 10^{-3}$  cm/GW (due to two-photon absorption, exciting wavelength is 800 nm) and  $3.6 \times 10^{-20}$  cm<sup>3</sup>/W<sup>2</sup> (due to three-photon absorption, exciting wavelength is 1064 nm). This new compound possesses strong fluorescence induced by two-photon absorption and obvious three-photon absorption optical limiting effects.

OCIS codes: 160.4330, 190.4180, 320.2250, 320.5390.

Organic molecules can simultaneously absorb two or more photons to be promoted to their excited states in the presence of intense laser pulses<sup>[1]</sup>. Because of a quadratic dependence of excitation on intensity, two-photon absorption (TPA) process could produce a spatially confined excitation useful for three-dimensional data storage and imaging. Two-photon absorption has received considerable attention recently because of the development of highly efficient two-photon-sensitive materials, leading to numerous technological applications<sup>[2-9]</sup>. These successes have created interest in exploring applications based on three-photon absorption (3PA)<sup>[10]</sup>. For a three-photon process, a longer excitation wavelength can be used, which enhances the penetrability of laser in materials. Also, the cubic dependence of the three-photon process on the input light intensity provides a stronger spatial confinement, so that a higher contrast in imaging can be obtained. However, the lack of the availability of dyes with sufficiently large cross-sections has made many practical applications appear unattainable. The development of molecules with large cross-sections requires more detailed studies on the structure-property relationships for nonlinear optics.

Fluorene derivatives have been considered as one of the best potential materials in the field of TPA science because of their unique properties involving the ease of increasing the effective conjugation length and polarizability of the molecule<sup>[11]</sup>. And over the past years, a series of asymmetric fluorene derivatives have been studied, since it is considered charge transfer between asymmetric substituents which can result in strong TPA<sup>[12]</sup>. But it is little systematically studied whether the symmetrical charge transfer fluorene derivatives can also enhance the

TPA. In addition, according to the previous reports<sup>[13,14]</sup> certain two-photon active organic molecules can be used for 3PA related applications. So the detailed studies on TPA and 3PA of symmetrical fluorene derivatives are becoming very significative.

In this letter, we report the observation of fluorescence behavior induced by TPA pumped with 140-fs pulses at 800 nm and obvious optical limiting effect induced by TPA pumped with 38-ps pulses at 1064 nm in a novel symmetrical charge transfer fluorene-based compound, which named 2,7-bis (4-methoxystyryl)-9, 9-bis (2-ethylhexyl)-9H-fluorene (abbreviated as BMOSF). The two- and three-photon absorption coefficients and the corresponding molecular absorption cross-section are presented.

Fluorene-based compound BMOSF was synthesized by the Heck reaction of 2, 7-dibromo-9, 9-diethylhexyl-9H-fluorene and 4-methoxystyrene using palladium acetate as a catalyst. The synthetic routes were shown in Fig. 1. In this molecular, the central fluorene moiety is attached through conjugation to an electron donating (D) pair of methoxy groups at both ends, forming a D- $\pi$ -D sequence. The resulting compound was confirmed by elemental analysis(C, H), mass spectrum and Fourier transform infrared spectrometer (FT-IR) spectra, respectively. The linear absorption spectrum and single-photon fluorescence spectrum were measured by using a Lambda 9 UV/VIS/NIR recording spectrophotometer and FP-6500 fluorescence spectrometer, respectively. The BMOSF solution in tetrahydrofuran (THF) with a concentration of  $1.5 \times 10^{-5}$  mol/L in a 1-cm-path quartz cuvette was used for both measurements.

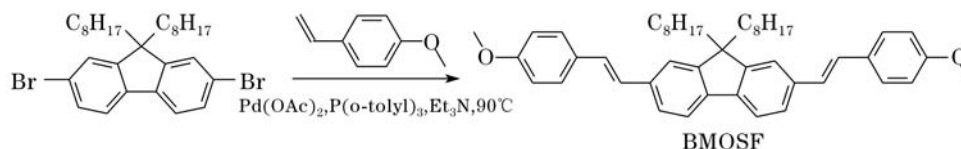


Fig. 1. The synthetic route of BMOSF.

The molecular TPA cross-section was measured by using an open aperture Z-scan system. TPA induced fluorescence spectrum of 1-cm-path BMOSF solution in THF with a concentration of 0.01 mol/L was measured by using imaging spectrography (Hamamatsu C5094). The pump laser beam came from a mode-locked Ti:sapphire laser operating at 800 nm with pulse duration of 140-fs, repetition rate of 1 kHz.

A 1-cm-path quartz liquid cell filled with BMOSF solution in THF with a concentration of 0.03 mol/L was used to observe the optical limiting effect induced by 3PA. The pump laser beam came from a Q-switched continuum Nd:YAG pulsed laser operating at 1064 nm with pulse duration of 38-ps, repetition rate of 10 Hz. The laser beam was separated into two beams by the beam splitter (BS). The weaker beam, detected by a photodiode PD1, was used to monitor the incident laser energy. The stronger beam, being focused into the sample by a 25-cm focal-length lens, acted as the exciting beam. The entire transmitted intensities through the sample were totally collected to a photodiode PD2. These two photodiodes were connected with a two-channel energy meter (Moletron EPM 2000) to record the input and output energies simultaneously. The input energy was adjusted from low to high by circumgyrating an attenuator, and corresponding output energy can be obtained.

In Fig. 2 curve (a) shows the linear absorption spectrum of BMOSF solution in THF. The influences from the quartz liquid cell and the solvent THF have been subtracted. One can find that there is a strong absorption band from 250 to 420 nm with a maximal absorption peak at 379 nm. No linear absorption is found from the wavelengths of 420 to 1200 nm. The two-photon energy of 800-nm radiation and three-photon energy of 1064 nm radiation just fall into the strong ultraviolet absorption, and therefore two-photon and three-photon absorption in this solution may be expected. Curve (b) shows the single-photon fluorescence spectrum excited at wavelength of 379 nm. From curve (b) it can be seen that the fluorescence band is from 380 to 600 nm with the peak wavelength of 418 and 438 nm. Curve (c) shows the TPA induced fluorescence spectrum excited at wavelength of 800 nm. From curves (b) and (c) one can see that there is a 30-nm red shift for the peak wavelength of two-photon induced fluorescence compared with that of single-photon

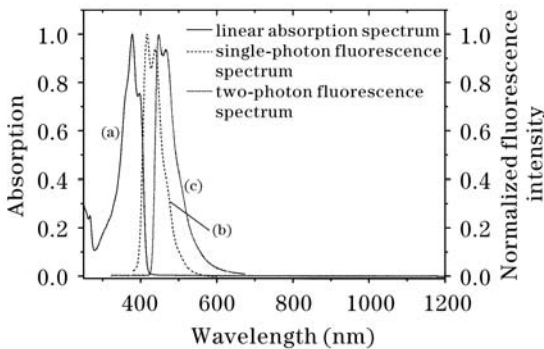


Fig. 2. Linear absorption spectrum ( $d_0 = 1.5 \times 10^{-5}$  mol/L), single-photon fluorescence spectrum ( $d_0 = 1.5 \times 10^{-5}$  mol/L) and two-photon fluorescence spectrum ( $d_0 = 0.01$  mol/L) of 1-cm-path BMOSF solution in THF.

induced fluorescence. This phenomenon can be explained by using reabsorption effect. Because there is a partial overlap between the linear absorption band and single-photon fluorescence band from 380 to 420 nm. This overlap will enlarge when the concentration becomes higher. The single-photon fluorescence spectrum was measured at low concentration ( $1.5 \times 10^{-5}$  mol/L), the reabsorption effect is not obvious and can be neglected. But the TPA induced fluorescence spectrum was measured at high concentration (0.01 mol/L). At this concentration level the reabsorption effect cannot be neglected. The intensity of short wavelength side of TPA induced fluorescence spectrum reduced greatly. So the peaks of two-photon fluorescence red shifted relative to the peaks of single-photon fluorescence.

Figure 3 shows the Z-scan data of BMOSF in THF measured in a 1-mm cell. In this figure, the normalized transmittance is reported as a function of the sample position ( $z$ ). Open apertures Z-scan system can be used to measure the TPA cross-section of TPA materials. The TPA coefficient can be calculated from the transmittance curves recorded by energy meter and computer. Based on theoretical consideration, for a temporally Gaussian pulse, the normalized energy transmittance can be given as<sup>[15]</sup>

$$T(z, s = 1) = \frac{1}{\sqrt{\pi}q_0(z, 0)} \int_{-\infty}^{+\infty} \ln(1 + q_0(z, 0))e^{-\tau^2} d\tau, \tag{1}$$

where  $q_0(z, t) = \beta I_0(t)L_{\text{eff}}/(1 + z^2/z_0^2)$ ,  $L_{\text{eff}} = (1 - e^{-\alpha L})/\alpha$ .  $\alpha$  is the linear absorption coefficient. For  $|q_0| < 1$ , the transmittance can be expressed in terms of the peak irradiance in a summation from that is more suitable for numerical evaluation

$$T(z, s = 1) = \sum_{m=0}^{\infty} \frac{[-q_0(z, 0)]^m}{(m + 1)^{3/2}}, \tag{2}$$

$(m = 0, 1, 2, 3, \dots)$ .

Once an open aperture Z-scan ( $s=1$ ) is performed, the nonlinear absorption coefficient  $\beta$  can be unambiguously deduced. The TPA can also be expressed by the molecular TPA cross-section  $\sigma_2$ . The relationship

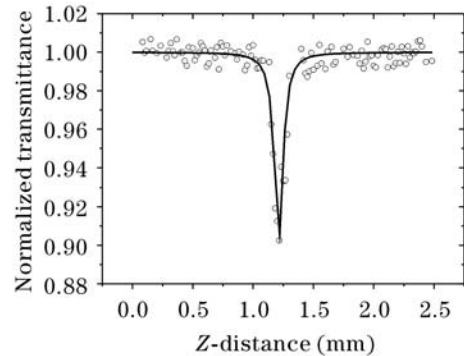


Fig. 3. Measured transmittance of a 1-mm-path BMOSF solution sample as a function of Z-distance using 140-fs, 800-nm laser pulses. The solid-line curve is obtained with a best-fitting parameter of  $\sigma_2 = 0.1 \times 10^{-20}$  cm<sup>4</sup>/GW.

between  $\beta$  and  $\sigma_2$  is

$$\beta = \sigma_2 N_0 = h\nu\sigma_2 N_A d_0 \times 10^{-3}, \quad (3)$$

where  $N_A$  ( $6.023 \times 10^{23}$ ) is Avogadro constant,  $h\nu$  is the photon energy,  $d_0$  is the concentration (in units of mol/L). Using the above equations, the TPA coefficient  $\beta$  and molecular TPA cross-section  $\sigma_2$  were calculated to be  $6.02 \times 10^{-3}$  cm/GW and  $2.5 \times 10^{-49}$  cm<sup>4</sup>·s/photon, respectively. Due to the influences of the quartz cuvette and the uncertainty of the incident intensity, the final result of  $\beta$  and  $\sigma_2$  of BMOSF has an experimental uncertainty of 15%.

Table 1 reports the TPA cross-section of BMOSF compared to those of the homologous representative literature examples measured in the femtoseconds' regime. AF50 (*N,N*-diphenyl-7-[2-(4-pyridyl) ethyl]-9, 9-di-n-decyl-9H-fluoren-2-amine) and AF250 (7-(7-benzothiazol-2-yl-9, 9-diethylfluoren-2-yl)-9, 9-diethylfluoren-2-yl) diphenylamine are two of the most representative asymmetrical TPA compounds so far reported<sup>[16]</sup>. It can be seen that compound BMOSF has the same order of magnitude compared with the TPA cross-section of these two examples, which indicates that symmetrical charge transfer fluorene derivatives can also obtain the high TPA activities.

Figure 4 shows the measured transmitted 1064-nm laser beam intensity versus the incident intensity. According to the basic theoretical consideration of 3PA, the intensity change of an excitation beam along the propagation direction ( $z$  axis) can be written as<sup>[10]</sup>

$$dI(z)/dz = -\gamma I^3(z), \quad (4)$$

**Table 1. TPA Cross-Section of Compound BMOSF in THF Compared to Literature Data of TPA Cross-Section of Different Compounds**

Compound	Pulse Laser		$\sigma_2$ (GM)	Solvent
	$\lambda$ (nm)	FWHM (fs)		
BMOSF	800	140	25	THF
AF50	796	150	22	THF
AF250	796	150	30	THF

1GM (Goppert-Mayer) =  $1 \times 10^{-50}$  cm<sup>4</sup>·s·photon<sup>-1</sup>.

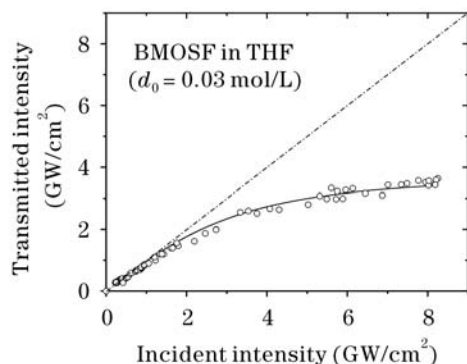


Fig. 4. Transmitted intensity as a function of the incident intensity for a solution sample of  $d_0 = 0.03$  mol/L (open circles). The solid curve is the theoretically fitted curve with a best-fit parameter of  $\gamma = 3.6 \times 10^{-20}$  cm<sup>3</sup>/W<sup>2</sup>. The propagation distance of the excitation 1064-nm laser beam within the sample was 1 cm.

where  $\gamma$  is the three-photon absorption coefficient of the given sample medium. The solution of Eq. (4) can be simply obtained as

$$T' = \frac{I(z)}{I_0} = 1/\sqrt{(1 + 2\gamma z I_0^2)}, \quad (5)$$

where  $I_0$  is the incident intensity of the excitation beam and  $z$  is the propagation distance within the sample medium. In Fig. 4 the open circles represent the measured data from the 1-cm-long solution sample with a concentration of  $d_0 = 0.03$  mol/L. The transmitted intensity dependent on the incident intensity clearly shows an optical power limiting behavior. The solid curve in Fig. 4 is the theoretically fitted curve given by Eq. (5) from the best-fit value of  $\gamma = 3.6 \times 10^{-20}$  cm<sup>3</sup>/W<sup>2</sup>. Based on the known  $\gamma$  value of the measured solution sample, the molecular absorption cross section  $\sigma'_3$  (in the units of cm<sup>6</sup>·s<sup>2</sup>) for given sample in solution is obtained by<sup>[17]</sup>

$$\sigma'_3 = \frac{\gamma}{N_A \cdot d_0 \times 10^{-3}} \left( \frac{hc}{\lambda} \right)^2. \quad (6)$$

Here,  $h(c/\lambda)$  is the energy of an incident photon at 1064 nm. So the intrinsic sample molecular  $\sigma'_3$  values can be easily estimated as  $\sigma'_3 = 70 \times 10^{-78}$  cm<sup>6</sup>·s<sup>2</sup> for BMOSF in THF (the final result of  $\sigma'_3$  of BMOSF has an experimental uncertainty of 15%). It can be easily found that this compound possess large 3PA cross sections in THF, which is 1.9 times greater than  $\sigma_3$  for the asymmetric homologous ( $\sigma'_3 = 37 \times 10^{-78}$  cm<sup>6</sup>·s<sup>2</sup>). This result indicates that symmetric intramolecular charge transfer from the methoxy groups to the conjugated core in the D- $\pi$ -D molecule helps to enhance 3PA. It is in agreement with Ref. [17].

Figure 5 shows the input intensity-dependent nonlinear transmittivity of compound BMOSF in THF with concentration of 0.03 mol/L. When the input intensity reaches to 8 GW/cm<sup>2</sup>, the limiting nonlinear transmissions  $T_{lim}$  can reach to about 40%. The solid line in Fig. 5 is the fitting curve by using the obtained parameter of  $\gamma = 3.6 \times 10^{-20}$  cm<sup>3</sup>/W<sup>2</sup>. The experimental data shown in Figs. 4 and 5 indicate that the BMOSF is a kind of promising optical power limiting materials induced by multiple-photon absorption in near infrared spectra regions.

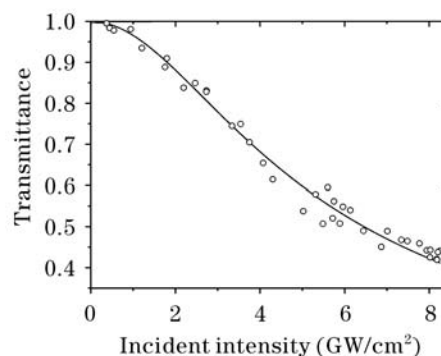


Fig. 5. Transmission change induced by 3PA versus input intensity of 1064 nm radiation.  $\gamma = 3.6 \times 10^{-20}$  cm<sup>3</sup>/W<sup>2</sup>,  $z = 1$  cm.

In conclusion, fluorene-based compound BMOSF is a kind of promising multi-photon absorption organic material. We investigated the nonlinear absorption of new compound BMOSF using 800- and 1064-nm radiation. The two- and three-photon absorption coefficients are measured to be  $6.02 \times 10^{-3}$  cm/GW and  $3.6 \times 10^{-20}$  cm<sup>3</sup>/W<sup>2</sup>, respectively, and the corresponding molecular absorption cross-section are as high as  $2.5 \times 10^{-49}$  cm<sup>4</sup>·s/photon (for fs pluses) and  $70 \times 10^{-78}$  cm<sup>6</sup> s<sup>2</sup> (for ps pluses). The results show that symmetrical charge transfer fluorene derivatives not only process high TPA activities, but also enhance 3PA in these fluorene derivatives. Large optical limiting effect induced by 3PA has also been demonstrated for this compound, when the input intensity reaches to 8 GW/cm<sup>2</sup>, the limiting nonlinear transmissions  $T_{lim}$  can reach to about 40%.

This work was supported by the National Natural Science Foundation of China (No. 60207005) and the Shanghai Science & Technology Development Foundation (No. 012261068). W. Ma's e-mail address is ma\_wenbo@mail.siom.ac.cn.

## References

1. M. Gopper-Mayer, *Ann. Phys.* **9**, 273 (1931).
2. W. Denk, J. H. Strickler, and W. W. Webb, *Science* **248**, 73 (1990).
3. J. Bewersdorf, R. Pick, and S. W. Hell, *Opt. Lett.* **23**, 655 (1998).
4. G. S. He, G. C. Xu, P. N. Prasad, B. A. Reinhardt, J. C. Bhatt, and A. G. Dillard, *Opt. Lett.* **20**, 435 (1995).
5. G. S. He, L. Yuan, P. N. Prasad, A. Abbotto, A. Facchetti, and G. A. Pagani, *Opt. Commun.* **140**, 49 (1997).
6. B. H. Cumpston, S. P. Ananthavel, S. Barlow, D. L. Daniel, J. E. Ehrlich, L. L. Erskine, A. A. Heikal, S. M. Kuebler, I.-Y. S. Lee, D. McCord-Maughon, J. Qin, H. Röckel, M. Rumi, X. L. Wu, S. R. Mader, and J. W. Perry, *Nature* **398**, 51 (1999).
7. D. A. Parthenopoulos and P. M. Rentzepis, *Science* **245**, 843 (1989).
8. J. H. Strickler and W. W. Webb, *Opt. Lett.* **16**, 1780 (1991).
9. J. D. Bhalwalkar, N. D. Kumar, C. F. Zhao, and P. N. Prasad, *J. Clin. Laser Med. Surg.* **15**, 201 (1997).
10. G. S. He, J. D. Bhawalkar, and P. N. Prasad, *Opt. Lett.* **20**, 1524 (1995).
11. O. K. Kim, K. S. Lee, H. Y. Woo, K. S. Kim, G. S. He, J. Swiatkiewicz, and P. N. Prasad, *Chem. Mater.* **12**, 284 (2000).
12. R. Kannan, G. S. He, L. X. Yuan, F. Xu, P. N. Prasad, A. G. Dombroskie, B. A. Reinhardt, J. W. Baur, R. A. Vaia, and L. S. Tan, *Chem. Mater.* **13**, 1896 (2001).
13. G. S. He, P. P. Markowicz, T. Lin, and P. N. Prasad, *Nature* **415**, 767 (2002).
14. D. Wang, C. Zhan, Y. Chen, Y. J. Li, Z. Z. Lu, and Y. X. Nie, *Chem. Phys. Lett.* **369**, 621 (2003).
15. S. B. Mansoor, A. A. Said, T. H. Wei, D. J. Hagan, and E. W. V. Stryland, *IEEE J. Quantum Electron.* **26**, 760 (1990).
16. J. Swiatkiewicz, P. N. Prasad, and B. A. Reinhardt, *Opt. Commun.* **157**, 135 (1998).
17. F. E. Hernández, K. D. Belfield, and I. Cohanoschi, *Chem. Phys. Lett.* **391**, 22 (2004).